Maximizing Singlet Fission in Organic Dimers: Theoretical Investigation of Triplet Yield in the Regime of Localized Excitation and Fast Coherent Electron Transfer†

Eric C. Greyson,‡ Josh Vura-Weis,‡ Josef Michl,*,§,|| and Mark A. Ratner‡

Department of Chemistry, Northwestern University, 2145 Sheridan Road, Evanston, Illinois 60208-3113, Department of Chemistry and Biochemistry, University of Colorado, 215 UCB, Boulder, Colorado 80309-0215, and Institute of Organic Chemistry and Biochemistry, Academy of Sciences of the Czech Republic, Flemingovo n. 2, 166 10 Prague 6, Czech Republic

Received: July 31, 2009; Revised Manuscript Received: December 20, 2009

In traditional solar cells one photon absorbed can lead to at most one electron of current. Singlet fission, a process in which one singlet exciton is converted to two triplet excitons, provides a potential improvement by producing two electrons from each photon of sufficient energy. The literature contains several reports of singlet fission in various systems, but the mechanism of this process is poorly understood. In this paper we examine a two-step mechanism with a charge transfer state intermediate, applicable when the initial excited state is localized. Density matrix theory is used to examine how various molecular properties such as orbital energies and electronic couplings affect singlet fission yield in the regime of fast, coherent electron transfer. Several promising chromophores are discussed and density functional theory is used to predict fission yield for each in the context of this mechanism. Finally, implications for chromophore design are discussed, and future experiments are suggested.

Introduction

Singlet fission (SF) was first discovered during an investigation of fluorescence quenching in anthracene crystals forty years ago.[1] Evidence that singlet excitation split into two triplet excitations was found in the specific magnetic field dependence of SF efficiency.[2−8] A number of more recent studies have identified singlet fission in other crystalline systems,[9−18] and in several polymers and small molecules,[19−33] although the fission mechanism may be difficult to identify conclusively.[34]

Photovoltaics could benefit from SF by yielding two charge carriers from a single absorbed photon,[35] and the phenomenon has recently attracted renewed interest. One of the first steps[36] was the identification of chromophores whose excitation energy into the lowest triplet level T_1 was roughly half the excitation energy into the first excited singlet energy level S_1, making SF thermodynamically favorable; additionally, the next triplet level T_2 was above S_1, making triplet−triplet annihilation endoergic. The energy levels of the individual chromophores are not the only factor governing SF yield, however, as several papers have shown very different yields for similar chromophores that are connected and electronically coupled in different ways.[21,25,26,29,30,37,38] In separate work, we used quantum chemistry to examine how coupling two isolated chromophores through a covalent bond to form a coupled chromophore pair would affect the free energy of SF and the electronic coupling matrix element.[39] One of the most important conclusions of this work is that stronger electronic coupling of the chromophores can lead to a pair in which SF is less exothermic, or more endothermic. Because electronic events are most likely to occur if they have large electronic matrix elements and are energetically favorable, there is probably a specific level of coupling that will optimize SF for any particular chromophore pair. While the understanding of SF is steadily growing, it is not yet clear exactly what balance of molecular properties will result in a dimer with the most efficient SF. The present paper deals with dimeric chromophores in which the lowest singlet excitation is localized and resides on one of the chromophores. As such, it is more applicable to chromophore pairs in solution or in glass than in crystals.

We examine a three-step mechanism consisting of an initial localized absorption on one chromophore followed by electron transfer from the excited chromophore to its partner, forming a charge transfer intermediate, followed by transfer of an electron of opposite spin in the opposite direction, resulting in a pair of charge-neutral triplets (if each chromophore is considered independent in the final state). We neglect the direct coupling of the initial state to the final state by the two-electron part of the Hamiltonian. Such Coulomb and exchange interaction is believed to be important in molecular crystals.[40−42] We analyze every possible electronic configuration in a four electron, four orbital model of a coupled chromophore pair and reduce the complexity of the problem to the most important configurations. The dynamics of the excitation are modeled with density matrix theory, assuming fast coherent electron transfer.

To predict SF yield in a series of dimeric chromophores, we (i) created a ten configuration dynamic model by analyzing SF with a four electron, four orbital basis, (ii) used electronic structure computations to evaluate both the energy of every state and electronic coupling element for a few promising chromophores, and (iii) applied the density matrix formalism to examine the evolution of the excitation over time for several test cases as well as for real molecules. Each of these three steps is discussed in further detail below.

Methods

Model System. We use the limit of two uncoupled chromophores to model SF in molecular coupled pairs We assume

† Part of the "Michael R. Wasielewski Festschrift".
‡ Northwestern University.
§ University of Colorado.
|| Academy of Sciences of the Czech Republic.

10.1021/jp907392q
Published on Web 02/25/2010

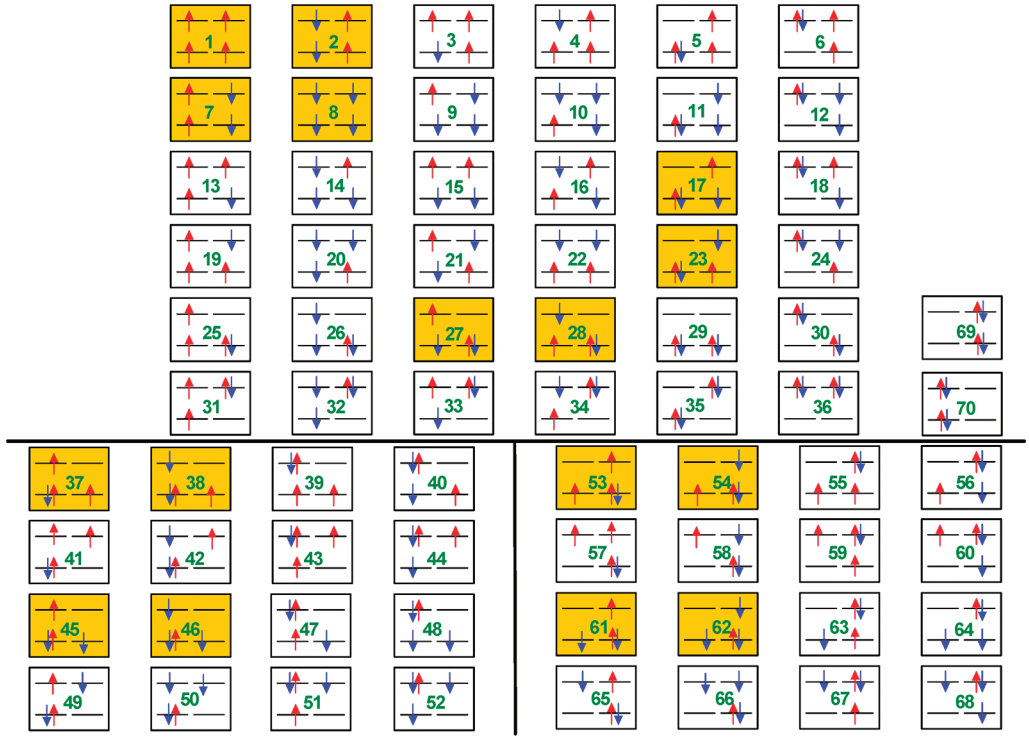

Figure 1. The 70 electron configurations in a 4-electron 4-orbital basis provided by the HOMO and the LUMO on each of a pair of chromophores. The lowest energy configurations are highlighted.

that the initial optical excitation is localized on one chromophore. To consider every possible mechanism for SF, we examine the 70 possible electron configurations that arise from four electrons in the four frontier molecular orbitals (HOMOs and LUMOs) of the uncoupled chromophore pair (Figure 1).

When both chromophores are neutral, each could be in one of six configurations, and so there are thirty six possible electron configurations representing a pair of neutral chromophores (labeled 1−36 above.) If a chromophore is a radical cation or anion (1 or 3 electrons in four frontier orbitals), there are only four possible electron configurations for each half. This provides an additional thirty two configurations (37−68 above), sixteen from a $A^{+\cdot}B^{-\cdot}$ combination and sixteen from the $A^{-\cdot}B^{+\cdot}$. Chromophores that are doubly charged only have one possible configuration, so our dimeric system has two double charge transfer configurations (69−70 above.)

We assume that only configurations close in energy to the initial configurations are likely to be accessed by a significant population during the lifetime of the excitation because of the energy gap law.[43] For singlet fission to be efficient it must be exothermic, and there are rare cases where it is strongly exothermic, so we assume the energy of one singlet should be about equal to twice the energy of a triplet. For solar cell applications, the singlet energy should be around 2.2 eV to optimize the photocurrent. Configurations such as 15, which contains two singlet excitations, or 19, with one singlet and one triplet excitation, can be easily eliminated from consideration, as we would estimate these to have energies of ∼4.4 or ∼3.3 eV (note that the terms "singlet" and "triplet" are not actually correct for some of the configurations in Figure 1, which are not eigenstates of the total spin operator, but we use these labels and figures for convenience).

Using this logic, we can reduce our system from seventy configurations to sixteen. We keep four configurations that are of S_1S_0 character (17, 23, 27, 28), four that have TT character

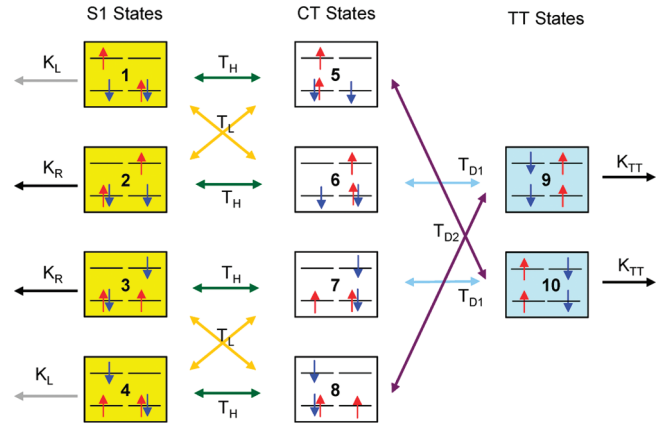

Figure 2. Allowed electron transfers in a 10-configuration system for SF, with definitive configuration numbering.

(1, 2, 7, 8), and eight single charge transfer (CT) configurations that are in their ground electronic state (37, 38, 45, 46, 53, 54, 61, 62).

In organics containing elements with atomic numbers less than ten, spin−orbit mixing is weak. Spin dipole−dipole coupling, which also has the ability to mix pure spin states and which is important for the understanding of magnetic field effects on triplet fusion and singlet fission in molecular crystals, will here also be neglected.[44] In addition, spin-flips in the CT state are expected to be slow.[45,46] Therefore, in discussing exciton fission we ignore configurations with overall spin projection ≠ 0 that can only be reached by spin−orbit coupling (1, 8, 37, 46, 53, 62). This yields a reduced ten-configuration scheme, as depicted in Figure 2, with configurations renumbered for convenience. Eight different one electron transfers can bring an excitation from one of the four S_1 configurations to one of the four CT configurations. Four of these steps involve one electron moving from the HOMO of one chromophore to the HOMO of the other, while the remaining four transitions in-

volve the transfer of an electron from the LUMO of one chromophore to the LUMO of the other. Such electron transfers can be referred to as "horizontal". The two TT configurations can be reached from the four CT configurations through "nonhorizontal" electron transfers, by either sending an electron from the LUMO of one chromophore to the HOMO of the other chromophore or vice versa.

In accordance with Koopmans' theorem, we make the approximation that orbital character is not affected by orbital occupancy. This means that every electron transfer from the HOMO of one chromophore to the HOMO of the other chromophore (or LUMO to LUMO) has the same matrix element, T_H (T_L). For an electron to move from a CT to a TT configuration there are four possible electron transfer steps, all of which involve a nonhorizontal transfer. These four can be split into two types: from left to right either HOMO to LUMO or LUMO to HOMO. If the two halves of a coupled chromophore pair are not the same, there are two different matrix elements for the two types of nonhorizontal electron transfer, T_{D1} and T_{D2}. Decay of the excited singlet and of the double triplet are considered the only ways for the excitation to leave the system in our model. Fluorescence, internal conversion, and intersystem crossing are possible forms of singlet decay. In the context of solar energy conversion, charge injection into an electrode or semiconductor nanoparticle (e.g., in a dye-sensitized cell) is another decay pathway for the excited singlet. In this work we will not attempt to distinguish between these S_1 decay pathways, and in Figures 4−8 we will refer to all of them together as "fluorescence". All of these S_1 decay pathways are included in the rate constants K_L and K_R in Figure 2. On the time scale of these simulations, the only triplet decay pathway is charge injection into the electrode due to (generally) long triplet lifetimes. Triplet decay is modeled with a single rate constant, while singlet decay is modeled with two separate decay constants for the two types of singlets (left and right localized singlet). In most cases the two singlet decay rates would be similar, but they could differ in a heterodimer or if the chromophore were bonded to the electrode differently for each half of the dimer. We suggest that this simple model captures the essential behavior of SF, although it would certainly be possible to add additional pathways (for example, direct coupling of the initial and final states by Coulomb and exchange interaction, spin flips due to spin−orbit coupling, spin dipole−dipole interaction, or CT state decay).

Electronic Structure Computations. We use electronic structure techniques to ascertain all of the parameters (energies and matrix elements) in the ten configuration model for several promising coupled chromophore pairs. We choose three such pairs and examine the effects of adding electron donating and withdrawing groups.

To model the dynamics of TT formation, we computed the energy of the isolated chromophores in their ground state S_0, first excited singlet configurations S_1, and first triplet T_1, as well as in their cation (C_1) and anion (A_1) ground configurations. All computations were done in the optimized ground state geometry because we assume for convenience that the dynamics are fast and coherent, preventing geometry relaxation (this and other effects of decoherence will be explored in future work). We continue to approximate the coupled chromophore pair energy as a sum of two independent chromophores. This approximation gives fairly accurate energies for the localized singlet and double triplet configurations of the dimers as long as the chromophores are weakly coupled, as all of the systems we study are. One advantage of this simplification is that the energy of many dimers in many different electronic configurations can be computed quickly. If the energy of any given pair is the sum of the energies of the two halves plus a correction term, one can compute energies for N^2 pairs in just N computations. The energy of the TT and the localized excited singlet configurations are generated by adding the energies of two independent chromophores in the appropriate electronic configurations:

$$E_{TT} = 2E_T - 2E_{S_0} \quad (1)$$

$$E_{S_1S_0} = E_{S_1} - E_{S_0} \quad (2)$$

where E_{TT} and $E_{S_1S_0}$ are the energy of the triplet pair and localized singlet coupled chromophore pair configurations, and E_T, E_{S_0}, and E_{S_1} are the independent chromophore triplet, ground configuration, and first excited singlet configuration energies. We note that this treatment (specifically eq 2) neglects exciton coupling between the monomers, which in the J-type geometry used here would lower the S_1 energy of the dimer vs that of the monomer.[47] The change in $E_{S_1S_0}$ caused by this exciton coupling is expected to be small compared to the difference between $E_{S_1S_0}$ and E_{TT} or $E_{C^+A^-}$ (see below), with little effect on the calculated fission yields.

To model accurately the energy of the CT states, we must account for the Coulombic stabilization from the two interacting halves:

$$E_{C^+A^-} = E_{C^+} + E_{A^-} - 2E_{S_0} \quad (3)$$

$$E^c_{C+A^-} = E_{C^+} + E_{A^-} - 2E_{S_0} - \Delta \quad (4)$$

where $E_{C^+A^-}$ and $E^c_{C^+A^-}$ are the uncorrected and corrected energy of a CT state of a dimer, E_{C^+}, E_{A^-}, and E_{S_0} are cation, anion, and ground energies of the monomer, and Δ is the correction energy. We use constrained DFT (CDFT)[48−50] to find the correction energy because the two charged chromophores are so close together. CDFT restricts the charge on each half of the dimer to +1 or −1 and iteratively adjusts the electron density of each half on the basis of the field from the other half.

$$\Delta = (E_{C^+} + E_{A^-} - 2E_{S_0}) - (E_{CDFT} - E_{CCPS_0}) \quad (5)$$

We run one CDFT computation for each coupled chromophore pair, and compare the CDFT energy (E_{CDFT}) to the neutral dimer energy, E_{CCPS_0} to find the correction term, Δ. The same correction is then applied to all variants of a given coupled chromophore pair with a given geometry. This allows a good estimate for the Coulombic stabilization without having to run a CDFT computation on every pair of chromophores.

The electronic matrix elements for hole and electron transfer, T_H and T_L, of the three basic coupled chromophore pairs have been previously investigated with density functional theory and Koopmans' theorem.[51] The half-energy level splitting method used to compute T_H and T_L can only be used directly to compute electronic matrix elements for orbitals that are close in energy. We thus cannot use the previous model to solve for the nonhorizontal (HOMO on one chromophore to LUMO on the other chromophore) electronic matrix elements. We instead rely on the Longuet−Higgins−Roberts approximation,[52−54] that

states that the electronic matrix element H_{ab} is proportional to the orbital overlap, S_{ab}.

$$H_{ab} = \langle \Psi_a | H | \Psi_b \rangle = kS_{ab} = k\langle \Psi_a | \Psi_b \rangle \quad (6)$$

We are examining the overlap of orbitals that arise from the independent chromophore Hamiltonians, but we will use them to estimate matrix elements for the coupled chromophore pair basis. To compute the overlap, S_{ab}, we split the geometry optimized dimer into two chromophores by cutting the connecting bond and hydrogen terminating each half. We then compute the wave function of the HOMO and LUMO for each chromophore. The (very small) overlap between the two HOMOs and between the two LUMOs is found by integrating over space, and we use these values and the known H_{ab} values from the half-splitting method (valid only when the two orbitals are close in energy) to compute the proportionality constant k. The integrated overlap S_{ab} for the nonhorizontal electron transfer is then used with this k, to find H_{ab} for nonhorizontal electron transfer. The same k computed for a coupled chromophore pair is used to compute matrix elements for the substituted versions of the chromophores from their overlap integrals.

All electronic structure computations were done with density functional theory (DFT) using the B3LYP functional with a 6-31G** basis set. Time dependent DFT (TDDFT) was used to evaluate the excited singlets for all systems, and constrained DFT (CDFT) was used to compute the energy of charge transfer dimer configurations. All computations were done using either QChem 3.0[55] or NWChem 5.0.[56,57] We used the CDFT module written by Van Voorhis and co-workers for implementation in NWChem 5.0.[48−50]

Time Evolution of Excitation. In this paper we examine coherent evolution of the excitation using density matrix formalism and a purely electronic Hamiltonian based on the ten configuration scheme discussed previously. To estimate the percent of the initial excitation that leaves the system through SF as opposed to other pathways, we introduce absorbing boundary conditions.[58] We investigate how the excitation can evolve in a coherent system with the Liouville−von-Neumann equation, adding in a term for dissipation.[59]

$$i\hbar(d\rho/dt) = [H_0,\rho] + [H_D,\rho]_+ \quad (7)$$

where H_0 is the Hamiltonian for the system, H_D is the dissipative matrix, and ρ is the density matrix. The Hamiltonian and dissipative correction matrix derived from our ten-configuration model are

$$H_0 = \begin{pmatrix}
E_{S_1S_0} & 0 & 0 & 0 & T_H & T_L & 0 & 0 & 0 & 0 \\
0 & E_{S_1S_0} & 0 & 0 & T_L & T_H & 0 & 0 & 0 & 0 \\
0 & 0 & E_{S_1S_0} & 0 & 0 & 0 & T_H & T_L & 0 & 0 \\
0 & 0 & 0 & E_{S_1S_0} & 0 & 0 & T_L & T_H & 0 & 0 \\
T_H & T_L & 0 & 0 & E_{AC} & 0 & 0 & 0 & 0 & T_{D2} \\
T_L & T_H & 0 & 0 & 0 & E_{CA} & 0 & 0 & T_{D1} & 0 \\
0 & 0 & T_H & T_L & 0 & 0 & E_{CA} & 0 & 0 & T_{D1} \\
0 & 0 & T_L & T_H & 0 & 0 & 0 & E_{AC} & T_{D2} & 0 \\
0 & 0 & 0 & 0 & 0 & T_{D1} & 0 & T_{D2} & E_{TT} & 0 \\
0 & 0 & 0 & 0 & T_{D2} & 0 & T_{D1} & 0 & 0 & E_{TT}
\end{pmatrix}$$

$$H_D = \begin{pmatrix}
-iK_L & 0 & 0 & 0 & 0 & 0 & 0 & 0 & 0 & 0 \\
0 & -iK_R & 0 & 0 & 0 & 0 & 0 & 0 & 0 & 0 \\
0 & 0 & -iK_R & 0 & 0 & 0 & 0 & 0 & 0 & 0 \\
0 & 0 & 0 & -iK_L & 0 & 0 & 0 & 0 & 0 & 0 \\
0 & 0 & 0 & 0 & 0 & 0 & 0 & 0 & 0 & 0 \\
0 & 0 & 0 & 0 & 0 & 0 & 0 & 0 & 0 & 0 \\
0 & 0 & 0 & 0 & 0 & 0 & 0 & 0 & 0 & 0 \\
0 & 0 & 0 & 0 & 0 & 0 & 0 & 0 & 0 & 0 \\
0 & 0 & 0 & 0 & 0 & 0 & 0 & 0 & -iK_{TT} & 0 \\
0 & 0 & 0 & 0 & 0 & 0 & 0 & 0 & 0 & -iK_{TT}
\end{pmatrix}$$

where H_0 is the Hamiltonian governing evolution within the ten-configuration manifold and H_D represents population leaving the ten configuration system by fluorescence, internal conversion, or injection. These decay rates are expressed in units of energy but may be converted to lifetimes via the energy−time uncertainty principle $\Delta E \Delta t = \hbar/2$. The system is set up with some initial density matrix ρ_0, where all of the population is equally distributed among the four local S_1 configurations and evolves in small finite time steps until all the population has left the system. At the end of the simulation we can examine the overall fission yield, based on how much population left the system via triplet pair decay as well as looking at the population of each determinant as a function of time. We interpret the percent of the excitation that has left the system by the triplet pair decay path to represent the percent of excitations in a given type of dimer that would undergo SF as opposed to other decay mechanisms.

We first run several simulations using artificial, but molecularly relevant, configuration energies E_n, electronic matrix elements T_n, and decay rates K_n to understand how variation within the parameter space affects fission yield in this model. We subsequently use parameters computed for real dimers to predict fission yields. The combination of these sets of data suggests both design parameters for molecular SF and systems for future experiments.

Results and Discussion

Electronic Structure. In this paper, we focus on one dimer of each of three different chromophores, as shown in Figure 3. 1,3-Diphenylisobenzofuran (**1**) was chosen as a representative of a biradicaloid system that is currently under experimental

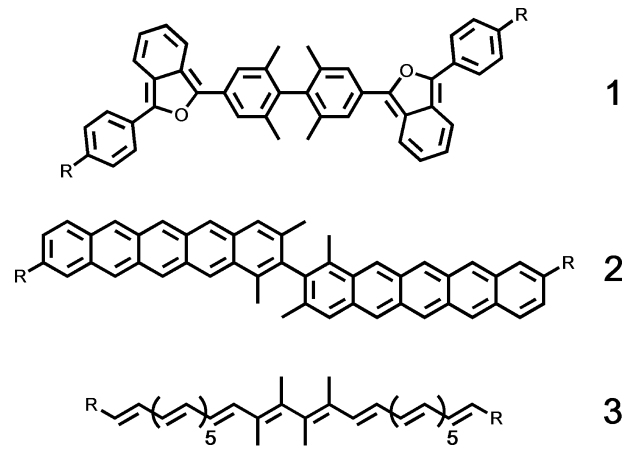

Figure 3. Structures of three promising coupled chromophore pairs. In addition to the parents (R = H), we also examine some variants where $R = NH_2$ or NO_2.

TABLE 1: Electronic Matrix Elements for Several Bare and Functionalized Dimers[a]

	T_H (eV)	T_L (eV)	T_{D1} (eV)	T_{D2} (eV)
1	0.068	0.068	0.066	0.066
2	0.068	0.082	0.056	0.056
3	0.065	0.059	0.065	0.065
*aa***1**	0.061	0.070	0.064	0.064
*an***1**	0.056	0.058	0.044	0.089
*nn***1**	0.066	0.034	0.046	0.046
*aa***2**	0.063	0.085	0.056	0.056
*an***2**	0.056	0.058	0.044	0.089
*nn***2**	0.066	0.056	0.051	0.051
*aa***3**	0.044	0.071	0.058	0.058
*an***3**	0.069	0.039	0.034	0.084
*nn***3**	0.096	0.022	0.047	0.047

[a] The prefixes aa, an, and nn are diamino, aminonitro, and dinitro functionalized variants.

TABLE 2: Energies of Electronic Configurations for Several Coupled Chromophore Pairs (in eV)[a]

	S_1S_0	S_0S_1	C^+A^-	A^-C^+	TT	Yield (%)
1	0	0	1.005	1.005	0.303	4
2	0	0	0.354	0.354	−0.240	24
3	0	0	0.595	0.595	−0.712	1
*aa***1**	0	0	0.988	0.988	0.384	2
*an***1**	0	−0.207	−0.144	1.823	0.286	42
*nn***1**	0	0	0.898	0.898	0.397	1
*aa***2**	0	0	0.345	0.345	−0.144	42
*an***2**	0	−0.089	−0.506	1.116	−0.169	46
*nn***2**	0	0	0.353	0.353	−0.105	42
*aa***3**	0	0	0.668	0.668	−0.222	7
*an***3**	0	−0.191	−0.484	1.674	−0.257	69
*nn***3**	0	0	0.712	0.712	−0.101	21

[a] The yield column will be discussed at the end of this section. The origin is taken as the higher of $E_{S_0S_1}$ and $E_{S_1S_0}$.

and theoretical examination.[36,38] Pentacene (**2**) was chosen as a representative acene. For both classes of structures, there are theoretical reasons to expect the observed favorable arrangement of energy levels, $E(S_1) \geq 2E(T_1)$. The polyene **3** was chosen for two reasons. Its SF would be unusually exothermic, and SF has been suggested to explain a high triplet yield reported in some protein-bound carotenoids.[21] Each of these three dimers is coupled in a similar manner, through a bond that would lead to direct conjugation if not for steric forces rotating the two chromophores nearly 90° out of plane from each other.

Each of the three primary dimers has a similar overlap integral and similar electronic matrix element owing to the similarity of the connections (Table 1). As one would expect, the electron donating and withdrawing groups affect the overlap, and hence matrix elements of each dimer. Most notable is the strong electron withdrawing property of the nitro groups, which leads to *nn*-dimers with very low T_L values. The nonhorizontal matrix elements are highly altered in the *an* dimers because electron transfer from the HOMO of the aminated chromophore to the LUMO of the nitrated chromophore has very small overlap, as both groups reduce the amplitudes of the frontier orbitals at the coupling positions, while the overlap for a transfer from the HOMO of the nitrated chromophore to the LUMO of the aminated chromophores is high since now the amplitudes are enhanced. This means the two nonhorizontal electron transfer matrix elements (as well as T_H and T_L) are very different in the *an* substituted dimers as opposed to many others where most of the electron transfer matrix elements are similar to each other.

Table 2 shows the energies of every relevant determinant in the ten configuration model for twelve dimers (the three primary dimers and several variants carrying electron donating and withdrawing groups). For unsubstituted species, **1** has the highest CT and TT state energies. The polyene **3** has the lowest TT energy, with significantly exothermic SF, while in **2** SF is slightly exothermic, and it has the lowest CT energies of the three. Derivatives of **1** and **2** carrying two amino or nitro substituents tend to have lower CT energies than the parent, while functionalized derivatives of **3** have higher energy CT configurations. The lower CT energies could result from the heteroatoms providing a good location for excess charge to reside, while it is possible that **3** is more stabilized by the functional groups in its local excited configuration than in the charge transfer. Almost every functionalized dimer has TT energy higher than the unfunctionalized version. This trend is expected and has been discussed previously.[39]

Time Evolution of Model Systems: Basic Model. To understand the type of dynamics that arise from this ten configuration coherent system, we first examine a simple case in detail. In this example, line 1 in Table 3, all ten configurations are assumed isoenergetic, and every matrix element is equal (0.027 eV). The decay rates K_L and K_R for both singlet exciton determinants and K_{TT} the triplet pair determinant are equal and set to 2.7×10^{-4} eV, which corresponds to a lifetime of 1.2 ps if singlet decay were the only pathway. The matrix elements are close to those of several promising dimers, and the decay rates are chosen to be on the order of very fast internal conversion events, while the state energies are chosen to be isoenergetic for simplicity. For a homodimer we assume that configurations 1−4 begin equally occupied.

As can be seen in Figure 4, population quickly leaves the S_1 configurations, enters the CT, and then moves into the TT. Under these conditions, the CT population reaches its first peak in less than 20 fs, and the TT population peaks in just under 30 fs. In Figure 4, and elsewhere, we use the term "fluorescence" to signify all the decay channels covered by the constants K_L or K_R in Figure 2. Unlike an isoenergetic two-configuration fully coherent system, where all the population would transfer to the second configuration before reversing direction, the TT population peaks at around 20% of the total population before all of the population flows back through the CT configurations to the S_1 configurations. Because of the many electron transfer pathways, the oscillatory nature of the populations is not simple. As expected, however, at all times, the four identical S_1 configurations have the same population, as do the four identical CT configurations, and the two identical TT configurations. After less than 2 ps, half the population of the system has exited through one of the decay channels, and after 5 ps more than 90% of the population has left. Because the decay rates are equal, the ratio of triplet pair injection to singlet decay is proportional to the ratio of the integrated populations of the TT and S_1 states over time. The ratio begins low because initially all population is in S_1, peaks as the TT population is first beginning to tail off (at 40 fs), and then settles on a very slowly rising curve, yielding ~11% fission at infinite time. Physically, this means that if a molecular system with these parameters (isoenergetic states, weak coupling and slow decay rates) were to be made, it would exceed any known experimental result for molecular SF. Note that in the language of many experimentalists this would be considered to be 22% yield, since two triplets are formed for each fission event. In this paper only the former terminology is used. To understand why the triplet yield is this promising in this example, as well as to see if we can get higher yields (perhaps even up to 100%), we do several other simulations with hypothetical molecular parameters below. These examples have been selected because they show some

TABLE 3: Simulations of Coherent Dynamics[a,b]

figure	T_H	T_L	T_{D1}	T_{D2}	K_{TT}	K_L, K_R	E14	E23	E58	E67	E90	% yield
4	0.027	0.027	0.027	0.027	0.00027	0.00027	0	0	0	0	0	11.0
5A	0.027	0.027	0.027	0.027	0.00054	0.00027	0	0	0	0	0	15.2
5B	0.027	0.027	0.027	0.027	0.00027	0.00054	0	0	0	0	0	7.5
6A	0.027	0.054	0.027	0.027	0.00027	0.00027	0	0	0	0	0	19.0
6B	0.027	0.027	0.027	0.054	0.00027	0.00027	0	0	0	0	0	22.5
6C	0.027	0.054	0.027	0.054	0.00027	0.00027	0	0	0	0	0	28.3
7A	0.027	0.027	0.027	0.027	0.00027	0.00027	0	0	0.081	0.081	0	11.0
7B	0.027	0.027	0.027	0.027	0.00027	0.00027	0	0	0.27	0.27	0	11.0
8A	0.027	0.027	0.027	0.027	0.00027	0.00027	0	0	0	0	0.027	11.0
8B	0.027	0.027	0.027	0.027	0.00027	0.00027	0	0	0.081	0.081	0.027	7.5
8C	0.027	0.027	0.027	0.027	0.00027	0.00027	0	0	0.27	0.27	0.027	2.5
S1A	0.054	0.054	0.054	0.054	0.00027	0.00027	0	0	0	0	0	11.0
S2A	0.027	0.027	0.027	0.027	0.00027	0.00027	0.027	0	0	0	0	15.3
S2B	0.027	0.027	0.027	0.027	0.00027	0.00027	0	0	0	0.027	0	16.0
S2C	0.027	0.027	0.027	0.027	0.00027	0.00027	0.027	0	0	0.027	0	20.8
S3A	0.027	0.027	0.027	0.027	0.0027	0	0	0	0	0	0	25.0
S3B	0.027	0.027	0.027	0.027	0.0027	0	N/A	0	0	0	0	50.0
S3C	0.027	0.027	0.027	0.027	0.0027	0	N/A, 0	N/A	N/A, 0	N/A	N/A, 0	100.0

[a] All couplings, decay rates, and energies are listed in eV. [b] Each row corresponds to a different simulation, and is identified by the number of a figure that provides more details. The electronic coupling matrix elements are listed first, then the decay rate constants, followed by the energies of the configuration (E14 stands for configuration 1 and 4), and finally the fission yield is listed. For additional detail on the simulations, see text.

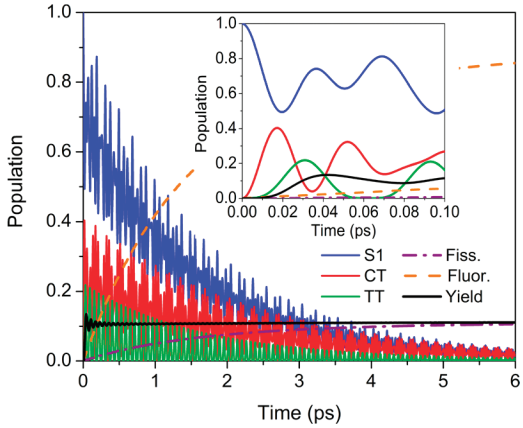

Figure 4. Coherent dynamics simulation of a basic isoenergetic system. Time dependence of the sum of all populations in S_1 (blue solid), CT (red solid), or TT (green solid) configurations, the percentage of the population that has left via fission (purple dash-dot) or fluorescence (orange dash) routes, and the percentage of population that has left the system through fission vs fluorescence (black solid). The inset shows the first 0.1 ps.

of the complex behavior of this interconnected ten configuration coherent system. An illustrative selection of simulations is summarized in Table 3 and discussed next.

Time Evolution of Model Systems: Effect of Decay Rates on SF. One of the easiest ways to increase or decrease fission yield within this model is to increase or decrease the ratio of the triplet pair and singlet decay constants, K_{TT}, K_L, and K_R. Using the parameters outlined above, if K_{TT} is doubled, the fission yield increases to 15%, while if K_L and K_R are instead doubled, the fission yield drops to 8% (Figure 5A,B, respectively). In both simulations the relative populations of each configuration are the same, as they are controlled by the matrix elements and energy levels of the configurations. The fission yield changes because a greater or lesser percent of the population in a given configuration exits per time period when the decay constants are changed. If all three decay rate constants are increased to 2.7×10^{-3} eV, the fission yield drops to 8%, because the combination of this short lifetime and the fact that all population begins in S_1 leads to a larger percent of singlet decay. If the decay rate constants are all lowered to 2.7×10^{-5} eV, however, the fission yield stays at 11%. As long as the decay rate is significantly slower than the rate of electron transfer, changing all of the decay constants proportionally does not affect fission yield (Figure 5C). Physically, this means that limiting nonradiative decay of singlets, singlet injection into an electrode, and fluorescence will be important for achieving high fission yields in a dye sensitized solar cell. It is worth noting that it is possible to increase K_{TT} and have fission yield decrease. The ideal triplet pair decay rate would match the rate at which population is being fed into the TT configurations. In the coherent isoenergetic example with all matrix elements equal, the ideal decay rate constant balances the feed-in rates to TT. A higher K_{TT} would actually decrease fission yield, as shown in the bottom of Figure 5C. This is not true for K_L and K_R, which always lead to increased singlet decay when increased. This difference exists because the population begins in S_1: if we artificially had all population begin in the TT states, the opposite would be true.

Time Evolution of Model Systems: Effect of Electronic Coupling Matrix Elements on SF. Previous research[38,39] has examined the strength of the electronic coupling between two chromophores in a coupled chromophore pair, since this coupling partly determines the rate of electron and energy transfer between the two halves. We examine how fission yield changes in the simple system shown in Figure 4 when the matrix elements are altered. Doubling every matrix element doubles the rate of oscillations, but the minimum and maximum populations for each configuration remain unchanged, and the overall fission yield is also unchanged (Figure S1, Supporting Information). This result is somewhat surprising, because a first guess would be that maximizing the electronic matrix element would be critical. In this example, the decay rates are far slower than the electron transfer rates, so the dynamic equilibrium between all states is established much quicker than decay regardless of the coupling in this regime. The fission yield is determined by the relative average populations of the S_1 and TT configurations and the ratio of the singlet and triplet pair decay rates. In both cases the average populations on S_1 and TT are the same, and the only difference is the rate at which population goes back and forth. The absolute magnitude of the electronic matrix elements is only important if there is a competing decay pathway that occurs on the same time scale

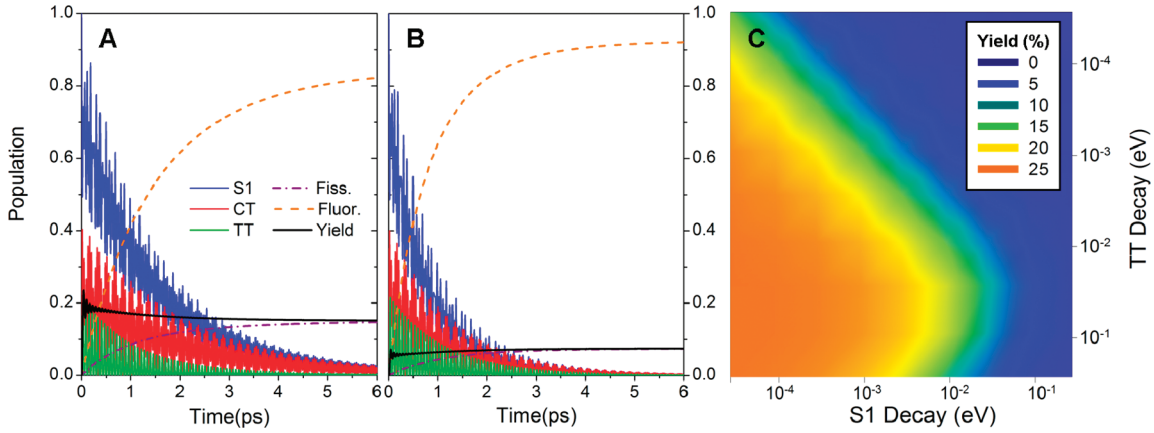

Figure 5. Coherent dynamics simulations showing the effects of doubling the TT decay (A) or S_1 decay (B) vs Figure 4. (C) shows the effect of a range of S_1 and TT decays on the fission yield.

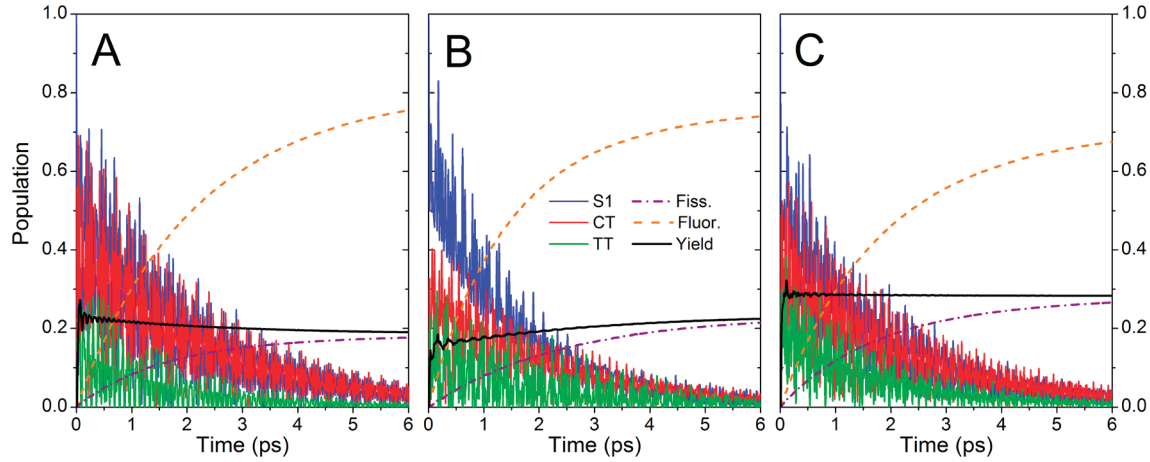

Figure 6. Coherent dynamics simulations of the effect of asymmetric electronic coupling matrix elements: (A) only T_L doubled; (B) only T_{D1} doubled; (C) T_L and T_{D1} doubled.

as electron transfer. If decay were very quick (<100 fs), significant population could decay from S_1 before any population reached TT. In this case larger electronic matrix elements would be important.

When only some of the electronic matrix elements are altered, however, the fission yield changes even when the decay rate is left the same ($K_L = K_R = K_{TT} = 2.7 \times 10^{-4}$ eV). If either the T_H or the T_L matrix element is doubled, but the other elements are unchanged from the initial simulation, the fission yield increases to ~19%. (Figure 6A). This increase in fission yield occurs because the destructive interference has been reduced, and some of the pathways (T_H vs T_L) from S_1 to CT are oscillating on a different time scale. The impact of destructive interference is discussed further in the Supporting Information. In a similar vein, if all matrix elements are the same, except for either T_{D1} or T_{D2}, then the yield jumps to 23% (Figure 6B). Additionally, the fission yield increases as the ratio of T_H to T_L increases to 2, but if the ratio of the matrix elements increases further, the fission yield drops again, to 15% when $T_H = 3T_L$. If both one of T_H or T_L and one of T_{D1} or T_{D2} are doubled while the other two remain the same, the fission yield jumps to 28%, as shown in Figure 6C (and if $K_L = K_R$ in this scenario, 100% fission yield is realized). In contrast to these beneficial modifications, if T_H and T_L are doubled but T_{D1} or T_{D2} is left unchanged, the fission yield drops to 5%. This is easy to understand, as the oscillations from S_1 to CT have sped up owing to the increased matrix elements, but the CT to TT transitions have not. These two transitions get out of phase, resulting in more population in S_1 and CT and less in TT compared to the case when all matrix elements are equal.

In terms of physical meaning, these examples provide several possible strategies for constructing an ideal dimer. Fission yield is increased when T_H and T_L are not equal. This will be the case when the dimer has more coupling (overlap) between the two chromophores in either the HOMO or LUMO. Previously examined molecules that displayed this tendency were donor−acceptor type structures. Fission yield is also increased when the two nonhorizontal electron transfer elements are not equal. To realize this, the dimer should be designed such that the $HOMO_{mol1}$−$LUMO_{mol2}$ overlap is better than the $HOMO_{mol2}$−$LUMO_{mol1}$ overlap, or vice versa. This could be done either by connecting two identical chromophores to each other in different locations or by binding two different chromophores together to make a heterodimer.

Effects of Nondegenerate State Energies on SF. Until now we have discussed highly artificial systems where all configurations are isoenergetic. This has let us study some of the behavior of our ten configuration coherent system but is not realistic for a real molecular system. We now examine the effects of changing the energy levels of various configurations using parameters similar to those in previous simulations, with all matrix elements set to 0.027 eV, and all decay rate constants equal to 2.7×10^{-4} eV. When the energies of both of the CT configurations are increased above that of the S_1 and TT configurations, there is no change in fission yield for small CT energies (Figure 7A). As the energy of the CT configurations

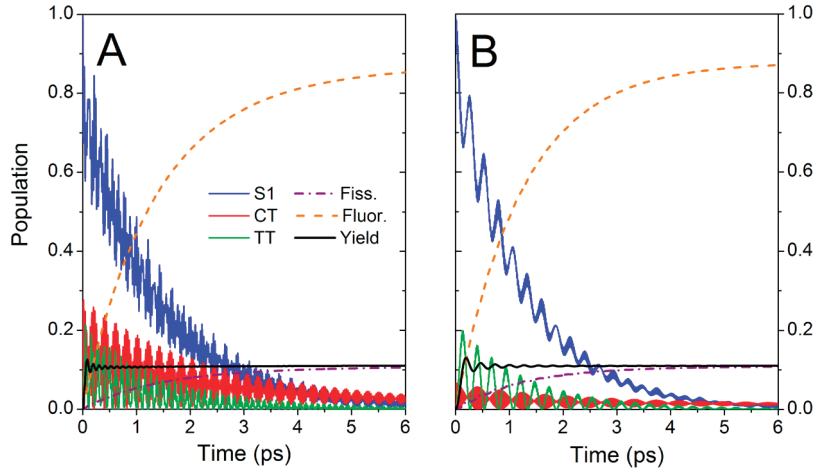

Figure 7. Coherent dynamics simulations of the effect of low (A) and high (B) CT barrier heights.

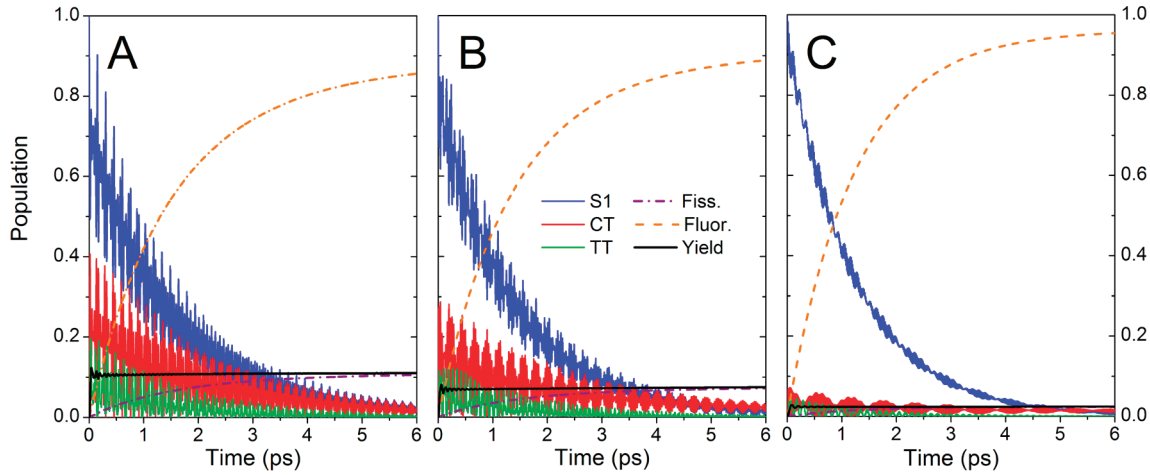

Figure 8. Coherent dynamics simulations of the effect of nondegenerate S_1 and TT energies with zero (A), low (B), or high (C) CT barrier heights.

moves further away from the S_1 and TT configurations, there are two noticeable differences in the population of various configurations over time. The CT configurations have a smaller population as the energy gap increases, and the major period of oscillation for all three types of configurations increases (Figure 7B). This is similar to coherent electron transfer between two configurations of different energies: as the energy gap increases, the period of oscillation increases, and the amount of population that is transferred decreases. Importantly, however, the relative populations of S_1 and TT are unaffected by this energy barrier. Given isoenergetic S_1 and TT configurations, the CT barrier height only affects the fission yield if the barrier height and singlet decay rate are such that all population leaves the system (from S_1) before one full period of S_1 to TT oscillations. At a barrier of 0.27 eV, the singlet would have to decay completely (by fluorescence or injection, for example) on the order of 90 fs to have the fission yield affected by the charge transfer energy barrier. If the barrier were 1.5 eV, the fission yield would decrease if the singlet exciton decayed in less than 750 fs. If both CT configurations are an equal energy below the S_1 and TT configurations instead of above them, the exact same behavior in population over time and overall fission yield is seen. In the regime of fast coherent electron transfer the energy difference between configurations (and matrix elements) determine the rate and magnitude of electron transfer, and the direction of energy change (uphill vs downhill) is irrelevant. This is typical of purely coherent superexchange phenomena and it should be noted that this is very different from how electron transfer rates depend on the energy in a Marcus-type rate picture.[60−62]

If S_1 and CT are isoenergetic but TT is shifted in energy, the fission yield decreases, regardless of whether the product TT is higher or lower in energy. From 11% fission yield in the isoenergetic case, the fission yields drops to 5% with a 0.081 eV offset, and <1% with a 0.27 eV offset. If CT and TT are isoenergetic, and S_1 is shifted instead, there is an identical drop in fission yield. If we combine an elevated CT configuration energy with a ΔG between the S_1 and TT configurations, the fission yield is worse than if there were the same ΔG but no CT barrier. In this case, the height of the CT barrier does affect fission yield. For a ΔG of 0.027 eV, the fission yield is 11% with no barrier, 8% with a 0.081 eV barrier, and 2.5% with a 0.27 eV barrier (Figure 8A−C, respectively). The main reason the barrier affects fission yield in this case is because the two electron transfer steps oscillate with different periods. While CT configurations at 0.081 eV and TT configurations at 0.027 eV lead to only 8% fission yield, if the CT barrier is put at −0.081 eV, the yield is 11%. When the barrier is positive, the energy difference between S_1 and CT is twice the gap between CT and TT, so the oscillations are very out of phase, whereas a negative barrier puts the oscillations of the S_1 to CT electron transfer step fairly close to the CT to TT electron transfer step, providing a higher fission yield.

In a heterodimer, it would be possible for the left and right localized S_1 and charge transfer configurations to be different in energy. If one of two sets of localized S_1 (configurations 1,4 vs 2,3) or CT (configurations 5,8 vs 6,7) configurations is not equal in energy to the other, the fission yield is typically increased. If either the left (or right) localized S_1 (or CT) configurations are increased in energy by 0.027 eV, and all other parameters are unchanged, the fission yield increases from 11% to 16% (Figure S2A,B, Supporting Information). If both one set of localized singlet configurations and one set of localized CT configurations are raised 0.027 eV, the fission yield increases to 21% (Figure S2C, Supporting Information). Changing the initial population of the system will change the fission yield in any simulation where the two localized singlets are not isoenergetic. If all of the population begins in the higher energy set of S_1 configurations in these examples, the yields are 11% and 15%. If all of the population begins in the S_1 configurations with lower energy (and isoenergetic with TT), the fission yields are 20 and 27%. In all of these cases the enhanced fission yield comes from symmetry breaking. In the unphysical case where $K_L = K_R = 0$, the fission yield is 50% if either the S_1 or CT configurations have broken symmetry, and 100% if both sets of configurations have broken symmetry (see discussion of interference effects in the Supporting Information).

From a molecular design point of view, these simulations suggest that heterocoupled chromophore pairs may be attractive targets because the two sets of localized S_1 and CT configurations will have different energies (although heteroCCP's will also have less favorable S_1-TT gaps). It is worth noting that unlike the case of the electronic matrix elements, even a very small breaking of the symmetry leads to a large increase in fission yield. Because of this, small differences in chromophores, such as electron donating or withdrawing groups, might suffice.

Lessons Learned. One of the major limitations for fission yield is the destructive interference that occurs when the system has high symmetry. This symmetry (and interference) is broken when left and right localized S_1 configurations and CT configurations have different energies, as is expected to be the case for heterodimers. The symmetry can also be broken by having the matrix elements T_H and T_L unequal, and T_{D1} and T_{D2} unequal. Additionally, this symmetry could be broken in a real system by dephasing or by a fluctuating environment. A second major factor in the fission yield is the relative decay rates of the TT and S_1. Because either half of a TT configuration can inject into the electrode first, while only the excited S_1 half of S_1S_0 can inject, it might be beneficial to link one-half of a dimer to the electrode more strongly than the other. If it is a heterodimer, by linking the higher energy localized S_1 to the electrode one might be able to retard singlet exciton injection into the electrode without adversely affecting triplet−triplet injection. The third major conclusion we can draw from these simulations is that coherent dynamics with no dephasing and zero temperature suggest that having the ΔG of SF as close to zero as possible will help fission yield (note that this is a stricter condition than the commonly noted $\Delta G < 0$ requirement). This conclusion agrees with the exponential gap law derived by Singh from consideration of the Coulomb and exchange interaction.[41]

Time Evolution of Real Molecules. Table 2 shows the fission yield for each of the twelve coupled chromophore pairs found using coherent dynamics within this ten configuration scheme. All of these simulations were run with $K_L = K_R = 2.7 \times 10^{-7}$ eV (1.2 ns lifetime), while $K_{TT} = 2.7 \times 10^{-4}$ eV (1.2 ps lifetime). The energy parameters in Table 3 were taken from Tables 1 and 2. These parameters are chosen to represent fluorescent decay of the localized singlets, and a quick triplet pair injection into an electrode. All three homodimers of **1** display very poor SF yield. They all have very high energy charge transfer configurations, and because of this very little population enters the CT configurations. The *an*-**1** chromophore has one CT configuration very close in energy to one of the S_1 configurations and, as a result, has a dramatically higher SF yield.

The most distinct trend in this data is that the dimers with TT energies closest to their lowest S_1 energies have the highest SF yield. In order of increasing absolute value of free energy of fission, the chromophores are ranked *an***3**, *an***2**, *nn***3**, *nn***2**, *aa2*, *aa***3**, **2**, **1**, *aa***1**, *nn***1**, *an***1**, and **3**. Only three of the dimers in this list are not in the place we would expect if we were to approximate that the only factor leading to high fission yield was a small absolute value of free energy of fission (energy of $TT-S_0S_1$). *aa***3** and *nn***3** would both be expected to have a greater SF yield based solely on their free energies of fission; however, their CT energy configurations are roughly twice as far away from S_1 and TT configurations as any of the more efficient dimers. *an***1** would be expected to be less efficient at SF based solely on the free energy of fission, but we note that it has a CT level far closer to its S_1 energy level than any other chromophore. This means more population transfers from the S_1 to the CT configuration, which limits singlet decay, and thus produces greater population in TT.

Overall, having a free energy of fission close to zero was the most important predictor of high fission yield, and having CT close in energy to S_1 and TT was the second most important factor. The electronic coupling matrix elements do not seem to be as important within the range that they cover in these molecules. This is what one would expect on the basis of the model simulations. We also note that the particular values of S_1 and TT decay chosen are unimportant when the relative yields between two coupled chromophore pairs with similar decay rates but different energetics are compared. As noted earlier, the fission yield is unchanged if the two decay rates are scaled by the same amount, as long as they are slower than the initial equilibration process between S_1, CT, and TT (Figure 5C).

Summary and Conclusion

For SF to be efficient within the framework of coherent, purely electronic dynamics, it is critical for the S_1 and TT states to be as close to isoenergetic as possible. If TT is not close in energy to the initial S_1 energy, the time average population in TT is very low, leading to low fission efficiency. In addition to this constraint on the free energy of the reaction, it is essential for CT to lie relatively close to the S_1 and TT energies for the population to be able to oscillate back and forth from S_1 to TT on a time scale comparable to or faster than excitation decay (as discussed earlier, we have neglected direct coupling of the initial and final states by direct Coulomb and exchange interaction). The magnitude of the various electron transfer matrix elements is not as important as the configuration energies, and thus dimer design should be done with energy in mind first. In most cases this will mean a relatively weak coupling is preferable, to prevent fission from being highly endothermic, but some chromophores, such as twisted polyenes, might perform better with stronger coupling because of low triplet energies. The energy of the CT intermediates can be controlled both by the choice of chromophore, where using biased chromophores provides a reduction in CT energy, and by controlling the Coulombic stabilization of a dimer CT configuration by moderating the distance between the charged chromophores. We find that dimers that combine these strategies to place as many energy levels as close together as possible are the ones that show the highest SF yields in the regime of coherent electron dynamics.

Several changes would be expected if dephasing were included in our model. Perhaps most importantly, the parasitic interference

that dramatically lowers singlet fission in some instances would disappear. We are currently investigating singlet fission using the (incoherent) Marcus electron transfer model and hope to discuss the similarities and differences of these two approximations.

Acknowledgment. We are grateful to the chemistry division of the ONR (N00014-05-1-0021) and to the DOE (1542544/XAT-5-33636-01, DE-FG36-08GO18017) for support of this work, and to Professor Abraham Nitzan and Dr. Sina Yeganeh for useful suggestions.

Supporting Information Available: Figures S1−S3: simulations of the effect of doubling the electronic coupling matrix elements; simulations of hetero-CCPs with nondegenerate energy levels; exploration of interference effects. Discussion of the effect of destructive interference on fission yields. This material is available free of charge via the Internet at http://pubs.acs.org.

References and Notes

(1) Singh, S.; Jones, W. J.; Siebrand, W.; Stoichef, B. P.; Schneider, W. G. *J. Chem. Phys.* **1965**, *42*, 330.
(2) Geacintov, N.; Pope, M.; Vogel, F. *Phys. Rev. Lett.* **1969**, *22*, 593–596.
(3) Geacintov, N. E.; Burgos, J.; Pope, M.; Strom, C. *Chem. Phys. Lett.* **1971**, *11*, 504–508.
(4) Katoh, R.; Kotani, M. *Chem. Phys. Lett.* **1992**, *196*, 108–112.
(5) Klein, G.; Voltz, R.; Schott, M. *Chem. Phys. Lett.* **1972**, *16*, 340–344.
(6) Merrifield, R. E.; Avakian, P.; Groff, R. P. *Chem. Phys. Lett.* **1969**, *3*, 155–157.
(7) Swenberg, C. E.; Van Metter, R.; Ratner, M. *Chem. Phys. Lett.* **1972**, *16*, 482–485.
(8) Yarmus, L.; Rosenthal, J.; Chopp, M. *Chem. Phys. Lett.* **1972**, *16*, 477–481.
(9) Arnold, S.; Alfano, R. R.; Pope, M.; Yu, W.; Ho, P.; Selsby, R.; Tharrats, J.; Swenberg, C. E. *J. Chem. Phys.* **1976**, *64*, 5104–5114.
(10) Arnold, S.; Whitten, W. B. *J. Chem. Phys.* **1981**, *75*, 1166–1169.
(11) Fleming, G. R.; Millar, D. P.; Morris, G. C.; Morris, J. M.; Robinson, G. W. *Aust. J. Chem.* **1977**, *30*, 2353–2359.
(12) Frankevich, E. L.; Lesin, V. I.; Pristupa, A. I. *Chem. Phys. Lett.* **1978**, *58*, 127–131.
(13) Groff, R. P.; Avakian, G. P.; Merrifield, R. E. *Phys. Rev. B* **1970**, *1*, 815–817.
(14) Jundt, C.; Klein, G.; Sipp, B.; Lemoigne, J.; Joucla, M.; Villaeys, A. A. *Chem. Phys. Lett.* **1995**, *241*, 84–88.
(15) Lopez-Delgado, R.; Miehe, J. A.; Sipp, B. *Opt. Commun.* **1976**, *19*, 79–82.
(16) Pope, M.; Geacintov, N. E.; Vogel, F. *Mol. Cryst. Liq. Cryst.* **1969**, *6*, 83–104.
(17) Vonburg, K.; Altwegg, L.; Zschokkegranacher, I. *Phys. Rev. B* **1980**, *22*, 2037–2049.
(18) Lee, J.; Jadhav, P.; Baldo, M. A. *Appl. Phys. Lett.* **2009**, *95*, 033301.
(19) Austin, R. H.; Baker, G. L.; Etemad, S.; Thompson, R. *J. Chem. Phys.* **1989**, *90*, 6642–6646.
(20) Dellepiane, G.; Comoretto, D.; Cuniberti, C. *J. Mol. Struct.* **2000**, *521*, 157–166.
(21) Gradinaru, C. C.; Kennis, J. T. M.; Papagiannakis, E.; van Stokkum, I. H. M.; Cogdell, R. J.; Fleming, G. R.; Niederman, R. A.; van Grondelle, R. *Proc. Natl. Acad. Sci. U.S.A.* **2001**, *98*, 2364–2369.
(22) Katoh, R.; Kotani, M.; Hirata, Y.; Okada, T. *Chem. Phys. Lett.* **1997**, *264*, 631–635.
(23) Kraabel, B.; Hulin, D.; Aslangul, C.; Lapersonne-Meyer, C.; Schott, M. *Chem. Phys.* **1998**, *227*, 83–98.
(24) Lanzani, G.; Cerullo, G.; Zavelani-Rossi, M.; De Silvestri, S.; Comoretto, D.; Musso, G.; Dellepiane, G. *Phys. Rev. Lett.* **2001**, *87*, 187402.
(25) Müller, A. M.; Avlasevich, Y. S.; Müllen, K.; Bardeen, C. J. *Chem. Phys. Lett.* **2006**, *421*, 518–522.
(26) Müller, A. M.; Avlasevich, Y. S.; Schoeller, W. W.; Müllen, K.; Bardeen, C. J. *J. Am. Chem. Soc.* **2007**, *129*, 14240–14250.
(27) Österbacka, R.; Wohlgenannt, M.; Chinn, D.; Vardeny, Z. V. *Phys. Rev. B* **1999**, *60*, R11253–R11256.
(28) Österbacka, R.; Wohlgenannt, M.; Shkunov, M.; Chinn, D.; Vardeny, Z. V. *J. Chem. Phys.* **2003**, *118*, 8905–8916.
(29) Papagiannakis, E.; Das, S. K.; Gall, A.; van Stokkum, I. H. M.; Robert, B.; van Grondelle, R.; Frank, H. A.; Kennis, J. T. M. *J. Phys. Chem. B* **2003**, *107*, 5642–5649.
(30) Papagiannakis, E.; Kennis, J. T. M.; van Stokkum, I. H. M.; Cogdell, R. J.; van Grondelle, R. *Proc. Natl. Acad. Sci. U.S.A.* **2002**, *99*, 6017–6022.
(31) Wohlgenannt, M.; Graupner, W.; Leising, G.; Vardeny, Z. V. *Phys. Rev. Lett.* **1999**, *82*, 3344–3347.
(32) Wohlgenannt, M.; Graupner, W.; Österbacka, R.; Leising, G.; Comoretto, D.; Vardeny, Z. V. *Synth. Met.* **1999**, *101*, 267–268.
(33) Zenz, C.; Cerullo, G.; Lanzani, G.; Graupner, W.; Meghdadi, F.; Leising, G.; De Silvestri, S. *Phys. Rev. B* **1999**, *59*, 14336–14341.
(34) Wohlgenannt, M.; Graupner, W.; Leising, G.; Vardeny, Z. V. *Phys. Rev. Lett.* **1999**, *83*, 1272–1272.
(35) Hanna, M. C.; Nozik, A. J. *J. Appl. Phys.* **2006**, *100*, 074510.
(36) Paci, I.; Johnson, J. C.; Chen, X. D.; Rana, G.; Popović, D.; David, D. E.; Nozik, A. J.; Ratner, M. A.; Michl, J. *J. Am. Chem. Soc.* **2006**, *128*, 16546–16553.
(37) Michl, J.; Nozik, A. J.; Chen, X.; Johnson, J. C.; Rana, G.; Akdag, A.; Schwerin, A. F. In *Organic Photovoltaics VIII*; Kafafi, Z. H., Lane, P. A., Eds.; Proceedings of SPIE; SPIE: Bellingham, WA, 2007; Vol. 6656, p 66560E1.
(38) Johnson, J. C.; Chen, X.; Rana, G.; Paci, I.; Ratner, M. A.; Michl, J.; Nozik, A. J. Manuscript in preparation.
(39) Greyson, E. C.; Stepp, B. R.; Cheng, X.; Schwerin, A. F.; Paci, I.; Smith, M. B.; Akdag, A.; Johnson, J. C.; Nozik, A. J.; Michl, J.; Ratner, M. A. *J. Phys. Chem. B*, DOI: 10.1021/jp909002d.
(40) Kral, K. *Czech. J. Phys. Sect. B* **1972**, *B 22*, 566–571.
(41) Singh, J. *J. Phys. Chem. Solids* **1978**, *39*, 1207–1209.
(42) Trlifaj, M. *Czech. J. Phys. Sect. B* **1972**, *B 22*, 832–840.
(43) Englman, R.; Jortner, J. *Mol. Phys.* **1970**, *18*, 145–164.
(44) Johnson, R. C.; Merrifield, R. E. *Phys. Rev. B* **1970**, *1*, 896–902.
(45) Reufer, M.; Walter, M. J.; Lagoudakis, P. G.; Hummel, B.; Kolb, J. S.; Roskos, H. G.; Scherf, U.; Lupton, J. M. *Nat. Mater.* **2005**, *4*, 340–346.
(46) Scott, A. M.; Miura, T.; Ricks, A. B.; Dance, Z. E. X.; Giacobbe, E. M.; Colvin, M. T.; Wasielewski, M. R. *J. Am. Chem. Soc.* **2009**, *131*, 17655–17666.
(47) Kasha, M.; Rawls, H. R.; El-Bayoumi, M. A. *Pure Appl. Chem.* **1965**, *11*, 371–392.
(48) Wu, Q.; Van Voorhis, T. *J. Phys. Chem. A* **2006**, *110*, 9212–9218.
(49) Wu, Q.; Van Voorhis, T. *Phys. Rev. A* **2005**, *72*, 24502.
(50) Wu, Q.; Van Voorhis, T. *J. Chem. Phys.* **2006**, *125*, 164105.
(51) Brédas, J. L.; Beljonne, D.; Coropceanu, V.; Cornil, J. *Chem. Rev.* **2004**, *104*, 4971–5003.
(52) Longuet-Higgins, H. C.; Roberts, M. d. V. *Proc. R. Soc. London, Ser. A, Math. Phys. Sci.* **1954**, *224*, 336–347.
(53) Venkataraman, L.; Klare, J. E.; Nuckolls, C.; Hybertsen, M. S.; Steigerwald, M. L. *Nature* **2006**, *442*, 904–907.
(54) Woitellier, S.; Launay, J. P.; Joachim, C. *Chem. Phys.* **1989**, *131*, 481–488.
(55) Shao, Y.; Molnar, L. F.; Jung, Y.; Kussmann, J.; Ochsenfeld, C.; Brown, S. T.; Gilbert, A. T. B.; Slipchenko, L. V.; Levchenko, S. V.; O'Neill, D. P.; DiStasio, R. A.; Lochan, R. C.; Wang, T.; Beran, G. J. O.; Besley, N. A.; Herbert, J. M.; Lin, C. Y.; Van Voorhis, T.; Chien, S. H.; Sodt, A.; Steele, R. P.; Rassolov, V. A.; Maslen, P. E.; Korambath, P. P.; Adamson, R. D.; Austin, B.; Baker, J.; Byrd, E. F. C.; Dachsel, H.; Doerksen, R. J.; Dreuw, A.; Dunietz, B. D.; Dutoi, A. D.; Furlani, T. R.; Gwaltney, S. R.; Heyden, A.; Hirata, S.; Hsu, C. P.; Kedziora, G.; Khalliulin, R. Z.; Klunzinger, P.; Lee, A. M.; Lee, M. S.; Liang, W.; Lotan, I.; Nair, N.; Peters, B.; Proynov, E. I.; Pieniazek, P. A.; Rhee, Y. M.; Ritchie, J.; Rosta, E.; Sherrill, C. D.; Simmonett, A. C.; Subotnik, J. E.; Woodcock, H. L.; Zhang, W.; Bell, A. T.; Chakraborty, A. K.; Chipman, D. M.; Keil, F. J.; Warshel, A.; Hehre, W. J.; Schaefer, H. F.; Kong, J.; Krylov, A. I.; Gill, P. M. W.; Head-Gordon, M. *Phys. Chem. Chem. Phys.* **2006**, *8*, 3172–3191.
(56) Bylaska, E. J.; de Jong, W. A.; Govind, N.; Kowalski, K.; Straatsma, T. P.; Valiev, M.; Wang, D.; Apra, E.; Windus, T. L.; Hammond, J.; Nichols, P.; Hirata, S.; Hackler, M. T.; Zhao, Y.; Fan, P.-D.; Harrison, R. J.; Dupuis, M.; Smith, D. M. A.; Nieplocha, J.; Tipparaju, V.; Krishnan, M.; Wu, Q.; Voorhis, T. V.; Auer, A. A.; Nooijen, M.; Brown, E.; Cisneros, G.; Fann, G. I.; Fruchtl, H.; Garza, J.; Hirao, K.; Kendall, R.; Nichols, J. A.; Tsemekhman, K.; Wolinski, K.; Anchell, J.; Bernholdt, D.; Borowski, P.; Clark, T.; Clerc, D.; Dachsel, H.; Deegan, M.; Dyall, K.; Elwood, D.; Glendening, E.; Gutowski, M.; Hess, A.; Jaffe, J.; Johnson, B.; Ju, J.; Kobayashi, R.; Kutteh, R.; Lin, Z.; Littlefield, R.; Long, X.; Meng, B.; Nakajima, T.; Niu, S.; Pollack, L.; Rosing, M.; Sandrone, G.; Stave, M.; Taylor, H.; Thomas, G.; van Lenthe, J.; Wong, A.; Zhang, Z. NWChem, a computational chemistry package for parallel computers, Version 5.1, Pacific Northwest National Laboratory, Richland, Washington 99352-0999, USA, 2007.
(57) Kendall, R. A.; Apra, E.; Bernholdt, D. E.; Bylaska, E. J.; Dupuis, M.; Fann, G. I.; Harrison, R. J.; Ju, J. L.; Nichols, J. A.; Nieplocha, J.; Straatsma, T. P.; Windus, T. L.; Wong, A. T. *Comput. Phys. Commun.* **2000**, *128*, 260–283.
(58) Bixon, M.; Jortner, J. *Adv. Chem. Phys.* **1999**, *106*, 35–202.
(59) Ter Haar, D. *Rep. Prog. Phys.* **1961**, *24*, 304–362.
(60) Beratan, D. N.; Onuchic, J. N.; Hopfield, J. J. *J. Chem. Phys.* **1987**, *86*, 4488–4498.
(61) Davis, W. B.; Wasielewski, M. R.; Ratner, M. A.; Mujica, V.; Nitzan, A. *J. Phys. Chem. A* **1997**, *101*, 6158–6164.
(62) Todd, M. D.; Nitzan, A.; Ratner, M. A. *J. Phys. Chem.* **1993**, *97*, 29–33.

JP907392Q